JOURNAL OF VIROLOGY, Oct. 2007, p. 10869–10878 Vol. 81, No. 20
0022-538X/07/$08.00+0 doi:10.1128/JVI.00542-07

Incorporation of High Levels of Chimeric Human Immunodeficiency Virus Envelope Glycoproteins into Virus-Like Particles[▽]

Bao-Zhong Wang,[1] Weimin Liu,[2] Sang-Moo Kang,[1] Munir Alam,[3] Chunzi Huang,[1] Ling Ye,[1] Yuliang Sun,[1] Yingying Li,[2] Denise L. Kothe,[2] Peter Pushko,[4] Terje Dokland,[2] Barton F. Haynes,[3] Gale Smith,[4] Beatrice H. Hahn,[2] and Richard W. Compans[1]*

Department of Microbiology and Immunology and Emory Vaccine Center, Emory University School of Medicine, 1510 Clifton Road, Atlanta, Georgia 30322[1]; Departments of Medicine and Microbiology, University of Alabama at Birmingham, 1530 3rd Ave. South, Birmingham, Alabama 35294[2]; Duke Human Vaccine Institute, Duke University School of Medicine, Durham, North Carolina 27710[3]; and Novavax, Inc., 9920 Belward Campus Drive, Rockville, Maryland 20850[4]

Received 14 March 2007/Accepted 21 July 2007

The human immunodeficiency virus (HIV) envelope (Env) protein is incorporated into HIV virions or virus-like particles (VLPs) at very low levels compared to the glycoproteins of most other enveloped viruses. To test factors that influence HIV Env particle incorporation, we generated a series of chimeric gene constructs in which the coding sequences for the signal peptide (SP), transmembrane (TM), and cytoplasmic tail (CT) domains of HIV-1 Env were replaced with those of other viral or cellular proteins individually or in combination. All constructs tested were derived from HIV type 1 (HIV-1) Con-S ΔCFI gp145, which itself was found to be incorporated into VLPs much more efficiently than full-length Con-S Env. Substitution of the SP from the honeybee protein mellitin resulted in threefold-higher chimeric HIV-1 Env expression levels on insect cell surfaces and an increase of Env incorporation into VLPs. Substitution of the HIV TM-CT with sequences derived from the mouse mammary tumor virus (MMTV) envelope glycoprotein, influenza virus hemagglutinin, or baculovirus (BV) gp64, but not from Lassa fever virus glycoprotein, was found to enhance Env incorporation into VLPs. The highest level of Env incorporation into VLPs was observed in chimeric constructs containing the MMTV and BV gp64 TM-CT domains in which the Gag/Env molar ratios were estimated to be 4:1 and 5:1, respectively, compared to a 56:1 ratio for full-length Con-S gp160. Electron microscopy revealed that VLPs with chimeric HIV Env were similar to HIV-1 virions in morphology and size and contained a prominent layer of Env spikes on their surfaces. HIV Env specific monoclonal antibody binding results showed that chimeric Env-containing VLPs retained conserved epitopes and underwent conformational changes upon CD4 binding.

In the life cycle of human immunodeficiency virus type 1 (HIV-1), assembly of the virion particle is an important step that is regulated by both viral and cellular factors (9, 24). The HIV Gag protein is sufficient for assembly, budding, and release from the host cell of virus-like particles (VLPs). Each particle is enveloped by a lipid bilayer derived from the host cell, and the envelope glycoprotein (Env) is incorporated into the particle during the process of assembly (10, 34). The Gag has a "late" (L) domain that promotes particle release by interacting with components of the cellular endosomal sorting pathway (15). Gag is also posttranslationally modified with an N-terminal myristate group, which is thought to target Gag to lipid rafts, thus aiding in assembly (25, 27).

The transmembrane (TM) and cytoplasmic tail (CT) domains of gp41 exert a key role in incorporation of the HIV-1 Env during HIV assembly. The TM and CT domains of HIV-1 and simian immunodeficiency virus Env have important effects on the orientation, surface expression, surface stability, and Env incorporation into particles (29, 35, 37). Previous studies suggest that specific regions in Env are involved in the interaction with Gag in assembly (9, 24); however, the detailed mechanisms that determine the incorporation of Env into VLPs remain to be determined.

In early studies, it was observed that HIV-1 Env is expressed and secreted very inefficiently in various expression systems, including yeast (1) and mammalian (6, 20, 21) cells. The substitution of the HIV Env signal peptide (SP) with that from honeybee mellitin was shown to promote higher-level expression and secretion of HIV-1 gp120 in insect cells (22). HIV-1 Env also has a CT sequence with over 150 amino acids (aa), whereas the glycoproteins of other viruses including mouse mammary tumor virus (MMTV), Lassa fever virus (LFV), baculovirus (BV) gp64, and influenza virus hemagglutinin (HA) have much shorter CT sequences from 7 to 43 aa in length. Interestingly, these viruses with shorter CT sequences incorporate their glycoproteins into virions at much higher levels than those found in HIV-1 (8). In the present study, we investigated the effects of various SP and TM-CT substitutions on the level of incorporation of HIV-1 Env into recombinant baculovirus (rBV)-derived Gag VLPs. We further compared the binding efficiency of well-defined antibodies against the HIV Env conserved epitopes in VLPs containing chimeric Env proteins.

* Corresponding author. Mailing address: Department of Microbiology and Immunology, Emory University School of Medicine, 1510 Clifton Road, Atlanta, GA 30322. Phone: (404) 727-5950. Fax: (404) 727-8250. E-mail: compans@microbio.emory.edu.

▽ Published ahead of print on 1 August 2007.

MATERIALS AND METHODS

Construction of chimeric Con-S Env genes. The Con-S ΔCFI gp145 gene, a derivative of the consensus HIV-1 group M ConS *env* gene which lacks the gp120-gp41 cleavage (C) site, the fusion (F) peptide, an immunodominant (I) region in gp41, as well as the CT domain (23) (H in Fig. 1), was obtained from

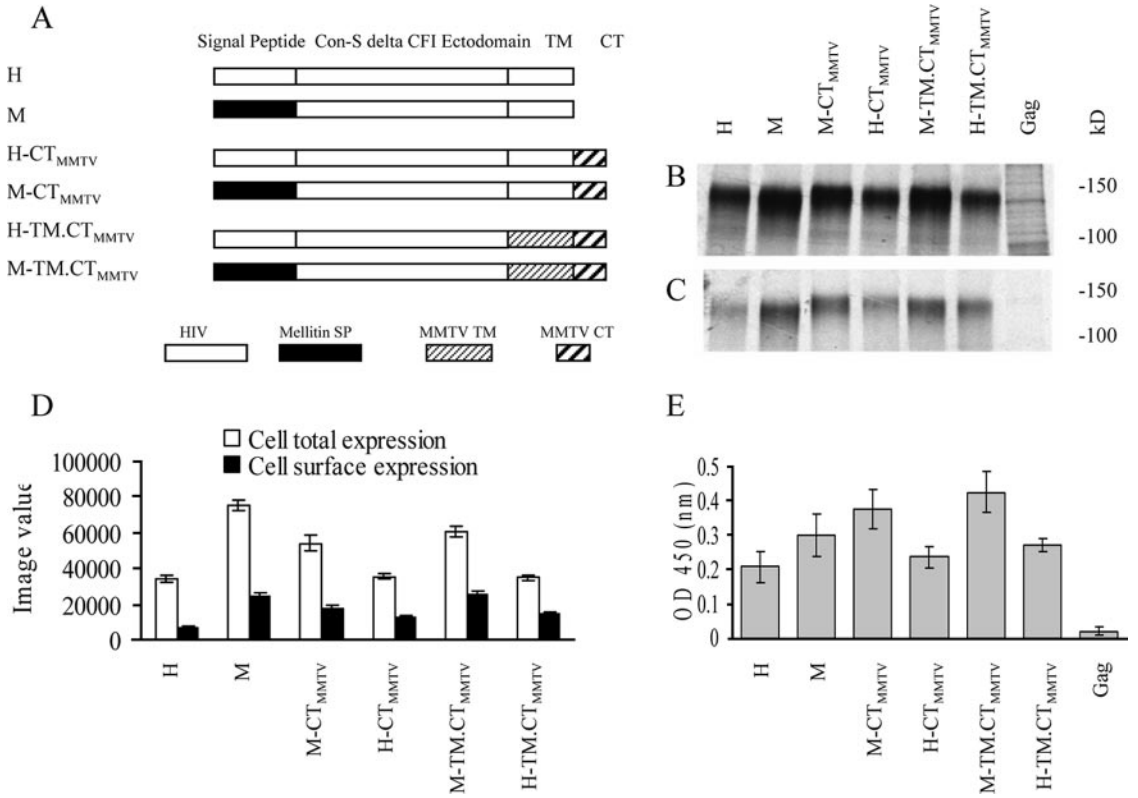

FIG. 1. Effects of SP substitution on total expression and cell surface expression of chimeric Con-S ΔCFI Env in Sf9 cells infected with rBVs. (A) Schematic diagram of modified chimeric HIV-1 Con-S ΔCFI Env. All components of the original HIV-1 gene are shown as empty boxes. The other components of chimeric segments are shown schematically by designations shown below. (B) Total cellular expression. (C) Cell surface expression. (D) Relative amounts in panels B and C quantified by phosphorimager analysis. Sf9 cells were infected with rBV at an MOI of 4 PFU/cell. At 48 h postinfection, the synthesized proteins were metabolically labeled with [^{35}S]methionine-cysteine, and cell surface proteins were identified by biotin labeling. Samples were resolved by SDS-PAGE, and the gel was dried and used for autoradiography and phosphorimager analysis. The image values were used for comparison of cellular total expression and cell surface expression. (E) CD4-binding activity of cell surface expressed Con-S chimeric proteins. Sf9 cells infected with rBV expressing chimeric HIV-1 Con-S constructs, at an MOI of 4 PFU/cell, were fixed, and the CD4 binding levels were determined by using a cell-based ELISA. Relative CD4-binding capacity is expressed as the optical density at 450 nm. (D and E) Representative data are shown from three independent experiments. Error bars represent the standard error.

Feng Gao (Duke University). All PCR primers used for generating chimeric constructs are listed in Table 1. Based on this H construct, the intermediate construct with the SP sequence and the stop codon deleted (sp-H) was generated by PCR using primers of F_{BamHI} and R_{SalI}. The PCR product was cloned into vector pBluescript II KS (pBlue) in the polylinker site with BamHI and SalI, and the resulting sp-H construct was used to generate other chimeric HIV-1 Env mutants. The mellitin SP (the sequence is in Table 2) with a 6-aa linker DPINMT was described previously (22, 26), and the corresponding DNA was synthesized through overlapping primer extension by PCR with the primers $F_{mellitin}$ and $R_{mellitin}$. This mellitin SP coding sequence was cloned into the sp-H construct at XbaI and BamHI sites (pBlue-pre-M). Then, a valine and a stop codon were introduced into pBlue-pre-M using the two primers F_{val}, and R_{val}, resulting in the construct pBlue-M (M in Fig. 1A).

To fuse the MMTV TM-CT to the chimeric HIV-1 Con-S ΔCFI *env* gene, the 73-aa-long MMTV Env (protein ID AAF31475) TM-CT-encoding gene (616 to 688 aa, the sequence is in Table 3) (18) was codon optimized, synthesized by primer overlapping extension PCR, and cloned into pBlue with EcoRI and ApaI (pBlue-MMTV-TM/CT). The HIV-1 Env ectodomain with the mellitin SP from pBlue-pre-M was amplified by using $F_{mellitin}$ and $R_{M\text{-}TM.CTMMTV}$ primers, and MMTV-TM/CT was amplified by using $F_{M\text{-}TM.CTMMTV}$ and R_{ApaI} primers. These two DNA fragments were fused by overlapping PCR extension (17), and the resulting construct was designated M-TM.CT$_{MMTV}$ (Fig. 1A). Similarly, the M-CT$_{MMTV}$ gene was constructed by overlapping PCR using pBlue-M and pBlue-MMTV-TM/CT as templates (M-CT$_{MMTV}$ in Fig. 1A). The primers used for this overlapping PCR were $F_{mellitin}$, $F_{M\text{-}CTMMTV}$, $R_{M\text{-}CTMMTV}$, and R_{ApaI}. To construct H-CT$_{MMTV}$ and H-TM.CT$_{MMTV}$ containing the natural HIV-1 Env

TABLE 1. Sequences of primers used

Primer	Sequence (5′–3′)
F_{BamH1}	GCAGGATCCGCCGAGAACCTGTG
R_{SalI}	GCTGTCGAC GATGGACAGCACGGC
$F_{mellitin}$	GGTTCTAGAATGAAATTCTTAGTCAACGT TGCC CTTGTTTTTATGGTCGTGTACATTTC
$R_{mellitin}$	GTGGGATCCGGTCATGTTGATCGGGTCCGCAT AGATGTAAGAAATGTACACGACCATAA
F_{val}	GTGCTGTCCATCGTCTAAGTCGACCTCGA GGGG
R_{val}	GAGGTCGACTTAGACGATGGACAGCACGGCG
$F_{M\text{-}TM.CTMMTV}$	GGTACATCAAGTTAAATCCATTAG
$R_{M\text{-}TM.CTMMTV}$	CTAATGGATTTAACTTGATGTACC
R_{ApaI}	CTGGGCCCCTATTAGGTGTAGG
$F_{M\text{-}CTMMTV}$	5-GTGCTGTCCATCGTCAAGAGCCTGGAC
$R_{M\text{-}CTMMTV}$	5-GTCCAGGCTCTTGACGATGGACAGCAC
pSP64U1	GGGGATCCACACAAGCAAGATGGTAA
Sgp160BsmBI-F	GCCGTCTCGCGGCCGAGAACCTGTGGGTGACC
pSP64BsmBI-R	GCCGTCTCGCCGCAAAGGCAGAATGCG
pConS145R	GGAATTCTTACACGATGGACAGCACGGCGAAC ACGATG
S145BsmBI	GCCGTCTCAACTTGATGTACCACAGCCAGTT
SP64BsmBI	GCCGTCTCAAGTTCATGTTTGGTCATGTAGTT
SP64CT-R	GGAATTCTTAATATTGTCTATTACGGTTTCTAA

TABLE 2. SP sequences of HIV-1 Env, mellitin, BV gp64, and chitinase

SP	Sequence (no. of aa)[a]	No. of positively charged residues
HIV-1 Env	M**R**V**R**GIQ**R**NCQ**H**LW**R**WGTLILG MLMICSA (29)	5
Mellitin	M**K**FLVNVALVFMVVYISYIYADP INMTGS (29)	1
BV gp64	MVSAIVLYVLLAAAA**H**SAFA (20)	1
Chitinase	MPLY**K**LLNVLWLVAVSNAIP (20)	1

[a] Letters in boldface represent positively charged residues.

SP, the XbaI and HindIII enzymatic fragments (SP plus partial ectodomain) of M-CT_{MMTV} and M-TM.CT_{MMTV} were replaced with the same enzymatic fragment from H (pBlue Con-S ΔCFI gp145), resulting in constructs designated H-CT_{MMTV} and H-TM.CT_{MMTV} (Fig. 1A).

A BV gp64 glycoprotein-derived chimeric Con-S ΔCFI Env gene was constructed by replacing the HIV-1 derived SP, TM and CT domains with the corresponding regions of the BV gp64 glycoprotein. The gp64 SP (20 amino acids) was amplified from pBACsurf-1 (EMD Bioscience, San Diego, CA) by using pSP64U1 and pSP64BsmBI-R. A Con-S ΔCFI gp145 gene fragment that lacked the cognate SP was amplified by using primers Sgp160BsmBI-F and pConS145R. These fragments were concatenated by using a BsmBI restriction enzyme site and cloned into pFastBac1. Gp64-ConSΔCFIgp140 was then amplified by using primers pSP64U1 and S145BsmBI, and the gp64 TM-CT domain was amplified from pBACsurf-1 by using primers SP64BsmBI and SP64CT-R. These two fragments were ligated at an internal BsmBI site which generated pFastBac1-gp64-ConSΔCFIgp140-gp64TM-CT. This chimeric *env* gene was cloned into pFastBac-Dual, which was modified by inserting the gp64 promoter downstream of the polh promoter, resulting in the construct designated B-TM.CT_{BV}.

To construct an influenza virus HA-derived chimeric Con-S ΔCFI Env gene, the HIV-1 SP was replaced with chitinase SP (the sequence is in Table 2) derived from *Autographa californica* nuclear polyhedrosis virus chitinase gene. The TM and CT domains of Con-S were replaced with the corresponding C-terminal region of influenza virus HA that contained putative TM and carboxy-terminal sequences derived from influenza A/Fujian/411/02 (H3N2) HA (the sequence is in Table 3). The chimeric gene was codon optimized for high-level expression in Sf9 cells and synthesized by primer overlapping extension PCR. The resulting PCR fragment was introduced into pFastBac1 transfer vector (Invitrogen) by using RsrII and NotI sites within the pFastBac1 polylinker. The identity of all constructs was confirmed by sequence analysis.

Generation of rBVs. The confirmed chimeric Con-S genes were subcloned into transfer vector pFastBac1 under the polyhedrin promoter. Recombinant BVs (rBVs) were generated by using a Bac-to-Bac expression system (Invitrogen) according to the manufacturer's instructions. Briefly, pFastBac1 plasmids containing chimeric Con-S ΔCFI HIV-1 *env* genes were transformed into DH10Bac competent cells (Invitrogen Life Sciences), white colonies were screened in LB media containing the antibiotics kanamycin (50 μg/ml), gentamicin (7 μg/ml), and tetracycline (10 μg/ml) and X-Gal (5-bromo-4-chloro-3-indolyl-β-D-galactopyranoside) and IPTG (isopropyl-β-D-thiogalactopyranoside). After three cycles of white colony screening, recombinant Bacmid BV DNAs (recombinant *Autographa californica* nuclear polyhedrosis virus) were isolated and transfected into Sf9 insect cells by using Cellfectin reagent (Invitrogen Life Sciences). Transfected culture supernatants were harvested, and plaques were purified. The expression of chimeric Con-S HIV-1 Env proteins from rBV-infected cells was confirmed by Western blotting.

For the generation of an HIV-1 Gag expressing rBV, we synthesized a codon usage optimized version of the 2002 consensus subtype B *gag* gene (GenBank accession number EF428978). For a similar rBV construct expressing the Lassa protein Z, its gene sequence encoding 99 aa, including 11 aa of an influenza virus HA epitope, was synthesized so that it is optimized for both mammalian and insect cell expression (DNA2.0, Inc., Menlo Park, CA) (14). Each of these synthetic genes was subcloned into transfer vector pFastBac1 under the polyhedrin promoter. These resulting pFastBac1 plasmids were used to generate rBVs according to the same procedure as that used for the generation of the chimeric Con-S Env rBVs described above. The protein expression from rBV-infected insect cells was confirmed by Western blot.

Cell surface expression assay. Sf9 cells were seeded in six-well plates at 10^6 cells/well. Recombinant BV infection, expression, and isotopic labeling were performed as described previously (31) with modification. In brief, Sf9 cells were infected with rBV at a multiplicity of infection (MOI) of 4 PFU/cell for 1 h at room temperature. The inoculum was removed and replaced with fresh Sf-900 II SFM medium (Gibco) plus 1% fetal bovine serum. At 48 h postinfection, virus-infected cells were placed in methionine and cysteine-free SF-900 II SFM medium for 45 min. Cells were then labeled with 250 μCi of [^{35}S]methionine-cysteine (Amersham)/ml for 4 h. Biotinylation of cell surface proteins was carried out as described previously (32). The final samples were loaded onto sodium dodecyl sulfate-polyacrylamide gel electrophoresis (SDS-PAGE). Gels were dried and then used for X-ray film exposure and phosphorimager analysis.

CD4-binding assay. Sf9 cells were seeded into 96-well plates at 2×10^4 cells per well and infected with rBVs as described above. Soluble CD4 (sCD4; acquired from the NIH AIDS Research and Reference Reagent Program) binding to cell surfaces was performed as described previously (19) with modifications. In brief, at 48 h postinfection, cells were washed three times with chilled phosphate-buffered saline (PBS) in an ice bath and fixed with 0.05% glutaraldehyde in PBS at 4°C for 1 h. After being washed with PBS, the cells were incubated with soluble human CD4 at a concentration of 5 μg/ml in PBS at room temperature for 1 h. After five washes with PBS, the amount of bound CD4 was determined with rabbit anti-human CD4 serum (1:10,000), followed by horseradish peroxidase (HRP)-conjugated goat anti-rabbit immunoglobulin G (IgG) polyclonal antibody (1:2000). Staining development was performed with a one-step substrate TMB (Zemed Labs), and the optical density at 450 nm was determined with an enzyme-linked immunosorbent assay (ELISA) reader (MTX Lab System).

VLP preparation. Sf9 cells were seeded in a 75-cm T-flask with 10^7 cells. After complete settling (about 1 h at room temperature), cells were coinfected with chimeric Env and Con-B Gag rBVs at MOIs of 8 and 2, respectively. After 72 h, media were clarified at 8,000 rpm for 25 min. VLPs were pelleted at 12,000 × *g* for 1 h through a 15% sucrose cushion, resuspended with PBS, and stored at 4°C for further analysis.

Determination of Env and Gag contents in VLPs. A sandwich ELISA was used for Env quantitation. Goat anti-HIV-1 gp120 polyclonal antibody (U.S. Biologicals) was used as a coating antibody and a mixture of monoclonal antibodies (MAbs), b12 and F425, was used as the detection antibodies. HIV-1 SF162 gp120 (NIH AIDS Research and Reference Reagent Program, catalog no. 7363) was used as the calibration standard. For Gag quantitation, a commercial HIV-1 p24 kit (Beckman Coulter) was used following the manufacturer's protocol. An sf2

TABLE 3. TM-CT sequences of Con-S Env, MMTV Env, BV gp64, LFZ glycoprotein, and influenza virus HA

Glycoprotein	Sequence	
	TM	CT
Con-S Env	IFIMIVGGLIGLRIVFAVLSIV	NRVRQGYSPLSFQTLIPNPRGPDRPEGIEEEGGEQDRDRSIRLVN GFLALAWDDLRSLCLFSYHRLRDFILIAARTVELLGRKGLRRG WEALKYLWNLLQYWGQELKNSAISLLDTTAIAVAEGTDRVIE VVQRACRAILNIPRRIRQGLERALL
MMTV Env	LNPLDWTQYFIFIGVGALLLVIVLMIFPIVF	QCLAKSLDQVQSDLNVLLLKKKKGGNAAPAAEMVELPRVSYT
BV gp64	FMFGHVVNFVIILIVILFLYCMI	RNRNRQY
LFV GP[a]	LGLVDLFVFSTSFYLISIFLHLIKIP	THRHIVGGPCPKPHRLNHKGICSCGLYKRPGVSVRWKR
Influenza virus HA	DWILWISFAISCFLLCVALLGFIMWAC	QKGNIRCNICI

[a] GP, glycoprotein.

p55 (NIH AIDS Research and Reference Reagent Program, catalog no. 5109) was used as a calibration standard.

Electron microscopy. For negative staining, VLP samples (5 to 10 μl) were applied onto a carbon-coated film. Five minutes later, the remainder was removed with filter paper. Then, 10 μl of 1% sodium phosphotungstate was applied onto the grid, and the samples were stained for 30 s. The staining solution was removed, and the grid was dried for 15 to 30 min at room temperature and observed by electron microscopy. Cryo-electron microscopy was performed as previously described (13). Briefly, 3 μl of sample at a total protein concentration of 1 mg/ml was loaded on Quantifoil holey film (Quantifoil Micro Tools, GmbH, Jena, Germany) and vitrified in liquid ethane. Micrographs were recorded on a Gatan Ultrascan 1000 charge-coupled device camera in an FEI Tecnai F20 electron microscope operated at 200 kV with a magnification of ×38,000 and a defocus of ~2.5 μm.

Surface plasmon resonance. Surface plasmon resonance assays were performed as described previously (23). In brief, a BIAcore 3000 instrument (BIAcore, Inc., GE Healthcare, Piscataway, NJ) was used for this assay, and data analysis was performed with BIA evaluation 4.1 software. Anti-gp120 MAb T8 (murine MAb that maps to gp120 C1 region provided by Pat Earl, Laboratory of Viral Diseases, National Institutes of Health, Bethesda, MD) or sCD4 in 10 mM sodium acetate buffer (pH 4.5) was directly immobilized to a CM5 sensor chip by using a standard amine coupling protocol for protein immobilization. An irrelevant murine IgG (Pharmingen, San Diego, CA) was used as a reference antibody surface for subtraction of nonspecific bulk responses. Prepared VLPs and controls were flowed over the CM5 sensor at 10 μl/min at 25°C. The binding of VLPs was followed by injection of 25 μl of MAb 17b (100 μg/ml). Binding of VLPs and subsequent MAb binding were monitored in real time at 25°C with a continuous flow of PBS (150 mM NaCl, 0.005 surfactant P20 [pH 7.4]) at 10 to 30 μl/min.

Epitope-specific antibody binding assay. A sandwich ELISA was used to determine the epitope-specific antibody-binding activity of VLP-incorporating Env. Ninety-six-well Nunc Maxisorb flat-bottom plates were coated overnight with 100 μl of goat anti-HIV gp120 polyclonal antibody at a concentration of 5 μg/ml. The VLPs were added at an amount of 0.05 μg for per well. After subsequent epitope-specific MAb binding, a goat anti-human IgG-HRP (1:5,000) was used for detection. Epitope-specific antibody-binding activity was expressed as the optical density at 450 nm.

RESULTS

Design of chimeric Env proteins. To determine the effects of the SP and TM-CT domains on the incorporation of Env into VLPs, three pairs of genes encoding chimeric Env were initially constructed for comparison (Fig. 1A). In pair I, the Con-S ΔCFI gp145 construct (H) is an HIV-1 group M consensus envelope gene with shortened variable loops, deletions of the cleavage site, the fusion domain, and an immunodominant region in gp41(ΔCFI) and a truncation of the cytoplasmic domain. The Con-S Env protein was demonstrated to elicit cross-subtype neutralizing antibodies of similar or greater breadth and titer than the wild-type Env proteins in guinea pigs (23). The ΔCFI form of the protein was reported to improve the ability to assemble into trimers and was shown to be an immunogen with enhanced capability to induce neutralizing antibodies in mice (5). Compared to the H construct, the M construct used the mellitin SP to replace the HIV-1 SP of H Env. The comparison of H and M was intended to reveal the effect of the heterologous mellitin SP, previously reported to lead to more efficient gp120 expression and secretion in an insect cell system (22). In pair II, the MMTV CT was added to the C termini of both H and M constructs, resulting in the chimeric constructs H-CT_{MMTV} and M-CT_{MMTV}. This modification was designed to explore the effect of a short heterologous CT on Env incorporation into VLPs and to compare the results with the CT truncated constructs in pair I. In pair III, the MMTV TM-CT was used to substitute for the corresponding regions in pair II, resulting in H-$TM.CT_{MMTV}$ and M-$TM.CT_{MMTV}$ constructs. These constructs were designed to examine a potential cooperative effect of homologous TM and CT domains on Env incorporation into VLPs. The effects of the mellitin SP were therefore assessed in three different formats. rBVs expressing all constructs were generated and confirmed to express the respective chimeric HIV-Env proteins in insect cells (Fig. 1B).

Effects of the SP on chimeric Env expression and CD4 binding. The effects of the mellitin SP on total Env synthesis and cell surface expression levels of chimeric Env were measured by radioactive metabolic labeling followed by surface labeling and immunoprecipitation. When rBVs containing chimeric genes were used to infect Sf9 insect cells, all three chimeric Env proteins with the mellitin SP substitution were expressed more efficiently in Sf9 cells (M, M-CT_{MMTV}, and M-$TM.CT_{MMTV}$ in Fig. 1B) compared to their corresponding counterparts with the natural HIV SP (H, H-CT_{MMTV} and H-$TM.CT_{MMTV}$ in Fig. 1B). Figure 1C compares the cell surface expression levels of the constructs, and Fig. 1D shows the relative quantities of bands in Fig. 1B and C by phosphorimager analysis. An enhancement by the mellitin SP substitution on the total expression of Env was observed in all constructs, independent of the changes in the CT or TM-CT domains. The chimeric Env without CT showed the highest level of total expression in Sf9 cells; however, the M with the CT deleted and M-$TM.CT_{MMTV}$ showed similar surface expression levels. Comparison of cell surface versus total expression levels indicated that M-$TM.CT_{MMTV}$ was the construct most efficiently transported to the cell surface as shown in Fig. 1D.

Env CD4-binding capability was also measured to examine whether the glycoprotein expressed on the cell surface was folded correctly. As shown in Fig. 1E, all chimeric Env proteins with the mellitin SP exhibited higher CD4-binding compared to their corresponding constructs with the HIV SP (M versus H, M-CT_{MMTV} versus H-CT_{MMTV}, and M-$TM.CT_{MMTV}$ versus H-$TM.CT_{MMTV}$ in Fig. 1E). The mellitin SP chimera with an MMTV TM-CT substitution exhibited the highest CD4-binding level (M-$TM.CT_{MMTV}$ in Fig. 1E). We observed a similar pattern when the cell surface expression (Fig. 1D) and the CD4 binding were compared, suggesting that the cell surface-expressed Env is folded into a correct conformation, at least for the CD4-binding domain. Similar results were observed in HeLa cells by using a vaccinia virus T7 polymerase-driven protein-expressing system (data not shown).

Effects of SP substitution on Env incorporation into VLPs. Since the chimeric Env proteins with mellitin SP substitution were expressed efficiently in Sf9 cells and exhibited higher surface expression, we determined whether these proteins could be incorporated more efficiently into VLPs containing the HIV-1 Gag protein. As shown in Fig. 2A, when 2 μg of the VLPs was analyzed by Western blotting, we observed that the mellitin SP chimeric Env with the CT deleted (M in Fig. 2A) was incorporated at levels threefold higher than the corresponding construct with the original HIV SP (H in Fig. 2A). Substitution of the MMTV CT or TM-CT also was found to enhance Env incorporation (M-CT_{MMTV} and M-$TM.CT_{MMTV}$ in Fig. 2A). For more detailed comparison, different amounts of H and M VLPs were resolved and compared by Western blotting with known levels of HIV-1 SF162 gp120. As shown in Fig. 2C, M Env incorporation was two- to

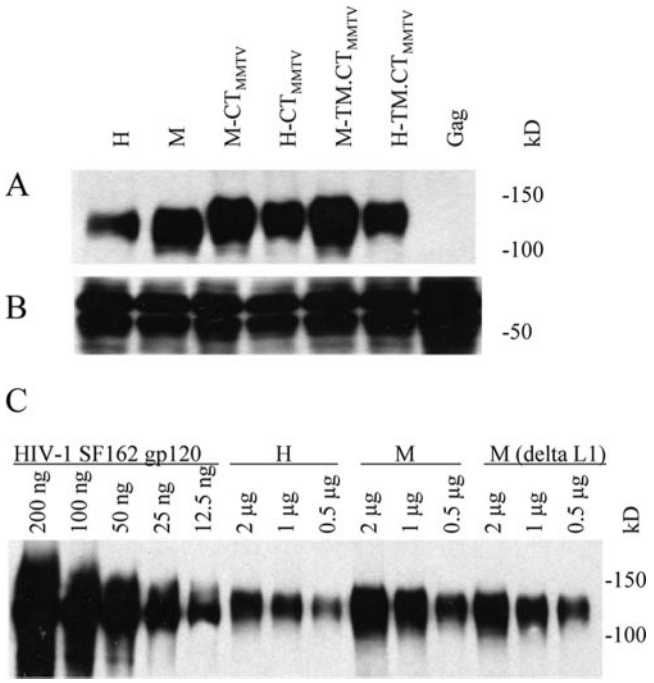

FIG. 2. Effect of SP substitution on the incorporation of Env into VLPs. VLPs were produced by coexpression of ConB Gag and chimeric Env constructs and concentrated by centrifugation through a 15% sucrose cushion. The protein concentration of resulting VLPs was determined with a Bio-Rad protein assay kit. (A and B) A portion (2 μg) of total VLP protein was used for Western blot analysis. In panel A, goat anti-HIV-1 Env gp120 polyclonal antibody was used as primary binding antibody; in panel B, mouse anti-HIV-1 Gag polyclonal antibody was used for ConB Gag detection. (C) Different amounts (μg/well) of HIV-1 SF162 gp120, H, M, and M(ΔL1) VLPs were loaded for Western blot analysis as indicated. The construct M-(ΔL1) was schematically depicted in Fig. 3B.

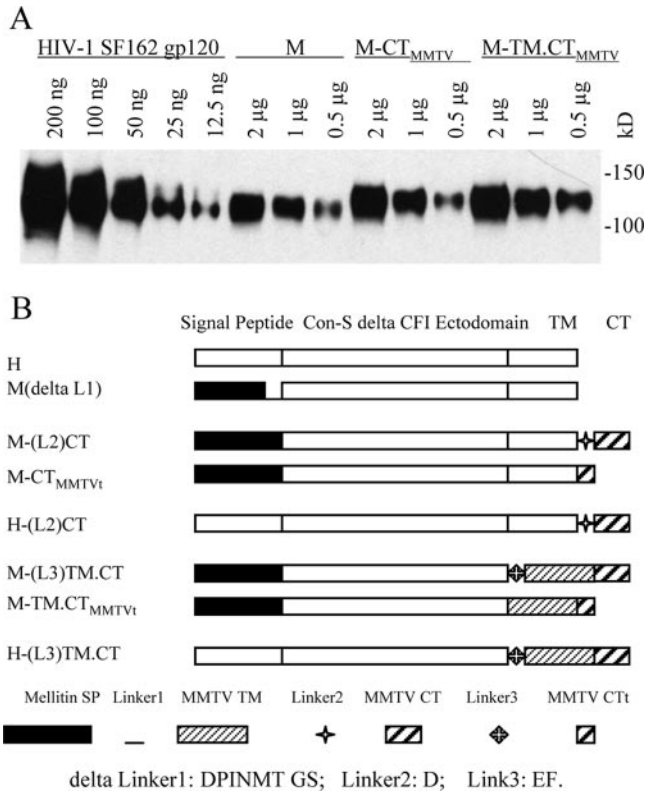

FIG. 3. Effects of MMTV TM, TM-CT, and flexible connecting regions on Env incorporation into VLPs. (A) Different amounts of HIV-1 SF162 gp120, M, M-CT$_{MMTV}$, and M-TM.CT$_{MMTV}$ were loaded for Western blot analysis as shown. (B) Schematic diagram of modified chimeric HIV-1 Con-S ΔCFI Env. The deleted linker 1 (L1) is DPINMTGS. L2 and L3 represent D and EF residues, respectively. For M-CT$_{MMTVt}$ and M-TM.CT$_{MMTVt}$, a 6-aa fragment, PRVSYT, was truncated at the C-terminal end of MMTV CT.

threefold higher than H Env (2, 1, and 0.5 μg of M versus 2, 1, and 0.5 μg of H).

Considering that the mellitin SP is a heterologous sequence and a conformational constraint may occur when it is fused to the Con-S surface domain, the initial M construct had a flexible linker, DPINMT GS, between the mellitin SP and Con-S surface domains (Fig. 1A). To evaluate the role of this linker, a chimeric Env gene, M(ΔL1) in Fig. 3B, was constructed in which the flexible linker was deleted. We found that the deletion of the flexible linker sequence resulted in a slight decrease of Env incorporation [2, 1, and 0.5 μg of M(ΔL1) versus those of M in Fig. 2C]. Also, because HIV Env expression was analyzed with BV-infected insect cells, the effects of BV gp64 and chitinase SP sequences were tested. Chimeric HIV Env constructs containing these SP substitutions did not show improvements in the levels of Env incorporated into VLPs compared to the wild-type HIV SP (data not shown).

Effects of the MMTV TM and CT sequences on Env incorporation into VLPs. To elucidate the role of MMTV TM and CT domains in incorporation of chimeric HIV-1 Env into VLPs, the mellitin SP-based constructs were fused with the MMTV CT (M-CT$_{MMTV}$) or with MMTV TM-CT (M-TM.CT$_{MMTV}$) as shown in Fig. 1A. For quantitative comparison, different amounts of VLPs were subjected to Western blot (Fig. 3A). As a standard for purified HIV-1 Env, various amounts of HIV-1 SF162 gp120 (12.5 ng to 200 ng) were used. This comparison clearly shows that M-CT$_{MMTV}$ is incorporated into VLPs more efficiently than the M construct (Fig. 3A). The M-TM.CT$_{MMTV}$ construct containing both MMTV TM and CT showed the highest levels of Env incorporation into VLPs.

We also investigated the effects of length of the MMTV CT domain on incorporating Env into VLPs. A 6-aa (PRVSYT) truncated MMTV CT construct (M-CT$_{MMTVt}$ and M-TM.CT$_{MMTVt}$ in Fig. 3B) was examined and found to have levels of Env in VLPs similar to those observed with the full-length MMTV CT (data not shown). The presence or absence of linkers between the junctions of HIV Env and MMTV CT or TM-CT was also compared to determine whether the presence of the linker would affect Env incorporation into VLPs. We did not observe differences in levels of Env incorporated into VLPs produced using the constructs containing a 1-aa linker (D) between HIV TM and MMTV CT [H-(L2)CT and M-(L2)CT in Fig. 4B] or a 2-aa (EF) linker between the junctions of HIV Env and MMTV TM [M-(L)TM.CT, H-(L)TM.CT in Fig. 3B] (data not shown).

Comparison of other chimeric HIV Env proteins with heterologous TM-CT domains. We further explored Env incorporation into VLPs with constructs having TM-CT domains derived from either influenza virus HA or BV gp64 proteins. As

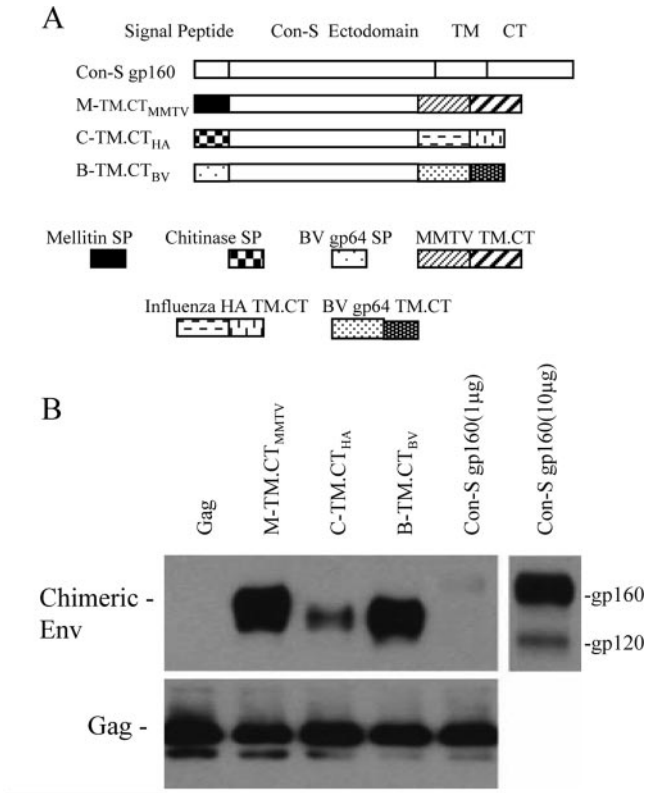

Env content*	----	8.7	3.6	7.9	0.81
Gag content*	17.4	13.1	14.7	13.7	15.5
Gag/Env Molar Ratio†	----	4.0	10.8	4.6	55.7

FIG. 4. Comparison of chimeric HIV-1 Env incorporation into VLPs. (A) Schematic diagram of additional chimeric HIV-1 Con-S Env constructs. B-TM.CT$_{BV}$, Con-S ΔCFI with SP and TM-CT domains derived from BV gp64; C-TM.CT$_{HA}$, Con-S ΔCFI with chitinase SP and influenza virus HA TM-CT domains. (B) In the upper left panel, 1 μg of M-TM.CT$_{MMTV}$, C-TM.CT$_{HA}$, B-TM.CT$_{BV}$, Con-S gp160, or HIV-1 Gag VLPs was analyzed by Western blotting. In the upper right panel, 10 μg of Con-S gp160 VLPs was loaded for the Western blot; in the lower panel, Env and Gag contents were quantitated by sandwich ELISA. *, μg/100 μg of the VLP protein. †, The molecular masses used for the ratio calculation were as follows: M-TM.CT$_{MMTV}$, C-TM.CT$_{HA}$, and B-TM.CT$_{BV}$, 145 kDa; Con-S gp160, 160 kDa; and Gag, 55 kDa.

diagrammed in Fig. 4A, one construct was generated to have chitinase SP and HA TM-CT (C-TM.CT$_{HA}$), and another contained the BV gp64 SP and TM-CT (B-TM.CT$_{BV}$). The incorporation of these chimeric Env into VLPs was compared to that of M-TM.CT$_{MMTV}$. The results in Fig. 4B demonstrate that all three of the chimeric constructs were found to be incorporated into VLPs at high levels, although the level of C-TM.CT$_{HA}$ was lower compared to the other two constructs. In contrast, the full-length Con-S gp160 was found to be incorporated into VLPs at very low levels under in the same conditions. The Con-S gp160 VLPs did not show detectable Env unless a 10-fold-higher quantity of VLPs was loaded for Western blot analysis, as shown in Fig. 4B (upper panel). Because Con-S gp160 is a full-length Env, it can be cleaved into gp120 and gp41, although the cleavage occurs at low levels because of limited expression of furin-like protease in insect cells. The data in the lower panel of Fig. 4B show that the Gag/Env molar ratios of MMTV-, HA-, and BV-derived chimeric Env VLPs were 4.0, 10.8, and 4.6, respectively, whereas the ratio for full-length Con-S gp160 VLP was 55.7, demonstrating that heterologous TM and CT domains have dramatic effects on enhancing the levels of incorporation of Env into VLPs.

We also constructed rBVs expressing chimeric Env proteins, H-CT$_{LFV}$ and H-TM.CT$_{LFV}$, as shown in Fig. 5A. Compared to H-CT$_{MMTV}$ and H-TM.CT$_{MMTV}$, H-CT$_{LFV}$ and H-TM.CT$_{LFV}$ have an LFV glycoprotein (GP)-derived CT or TM-CT substitution, respectively. As shown in Fig. 5B, the two chimeras were expressed efficiently in Sf9 cells infected with rBV recombinants when cell lysates were analyzed by Western blotting. However, when the two chimeras were used for VLP production with either the Con-B Gag or the Lassa matrix (Z) protein (LFV Z), the resulting VLPs did not contain any detectable Env. As a positive control, M-TM.CT$_{MMTV}$ VLPs showed high levels of Env with either Con-B Gag or LFV Z, demonstrating that both matrix proteins function well in VLP production and Env incorporation (Fig. 5B and C). Also, the wild-type LFV glycoprotein is effectively incorporated into Z-derived VLPs (Fig. 5D), indicating that the TM/CT of LFV GP are able to function in assembly of VLPs containing the LFV Z protein. This result shows that there are specific requirements involved in HIV Env incorporation in the assembly of VLPs, which are not fulfilled by the LFV TM/CT sequences.

Electron microscopy of Env enriched VLPs. The structure and size of VLPs containing chimeric HIV-1 Env were examined by electron microscopy. Conventional negative staining showed roughly spherical particles with sizes similar to those of HIV virions (Fig. 6A). Membrane fragments were also observed, which probably resulted from disrupted particles. Although the particles are slightly deformed, Env spikes are visible in selected images, as shown in the inset. These features were confirmed by cryo-electron microscopy, which has the advantage of preserving the native form of VLP structures without dehydration and staining artifacts (13). Cryo-electron microscopy of VLPs incorporating the M-TM.CT$_{BV}$ chimeric Env protein revealed a major population of spherical particles with a mean diameter of 145 ± 8 nm (Fig. 6B). These particles clearly showed the lipid bilayers and radial pattern characteristic of immature HIV-1 cores (16). A subset of small particles (<80 nm), a number of BV virions, and nucleocapsids and larger vesicular structures were also observed. The VLPs and most of the other membranous structures were studded with mushroomlike protrusions, presumed to represent the Env trimers. Chimeric VLPs incorporating TM-CT domains from influenza virus HA or MMTV were similar in appearance (not shown). VLPs containing the native HIV Env protein show fewer surface protrusions (2). In contrast, VLPs containing only the Gag protein were predominantly smooth surfaced, not coated with spikes like the VLPs containing chimeric Env proteins (Fig. 6C). A minor fraction of these particles showed some spikes, which may consist of the BV glycoprotein gp64.

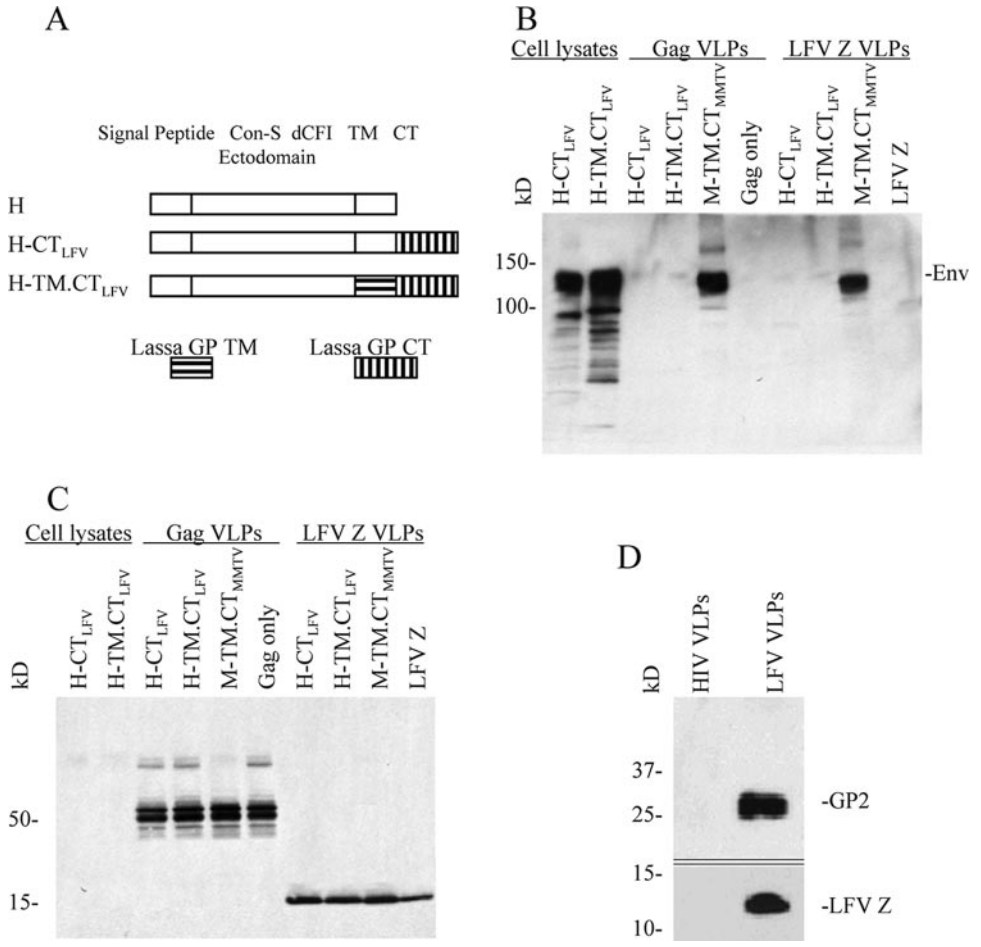

FIG. 5. Western blot analysis of VLPs produced using LFV GP-derived CT or TM-CT chimeric Env proteins. (A) Schematic diagram of chimeric Con-S Env fused with LFV GP-derived CT/TM-CT. The coding sequence for the LFV glycoprotein CT (LFV GP aa 450 to 491) or TM-CT (LFV GP aa 427 to 491) was fused to that of the C-terminal end of Con-S ΔCFI. (B) Western blot of protein expression in cell lysates and VLPs probed using goat anti-HIV-1 gp120 antibody. (C) Western blot of VLP matrix proteins (1 μg/well) released in VLPs probed with a mixture of mouse anti-HIV-1 Gag and anti-Lassa Z antibody mixture. (D) LFV Z VLPs, which incorporated the LFV GP. LFV VLPs were harvested from the culture supernatants of insect cells infected with rBVs expressing LFV GP and Z and resolved by SDS-PAGE, and the blot was probed with antibodies specific to LFV GP2 and Z. Each lane contains 5 μg of VLPs.

Antigenic properties of Env-enriched VLPs. To determine whether the correct conformation and conserved epitopes are formed and accessible to neutralizing antibodies, we applied either sCD4 or MAb T8 to a sensor chip to capture chimeric VLPs, and the captured VLP signals were recorded. Subsequently, MAb 17b binding to its CD4-induced epitope was determined. As shown in Fig. 7, chimeric VLPs or SF162 gp120 were captured by either sCD4 or T8, but essentially no binding was observed by Gag VLPs lacking the Env protein (Fig. 7A and B). VLPs were induced to bind MAb 17b only after binding to CD4, but not T8, demonstrating that chimeric Envs in VLPs undergo conformational changes induced by CD4 (Fig. 7C).

We also examined the capacity of chimeric VLPs for binding other well-defined antibodies by sandwich ELISA compared to that of full-length Con-S gp160. We found that VLPs containing Con-S ΔCFI gp145 M-TM.CT$_{MMTV}$ and M-CT$_{MMTV}$ show higher antibody binding capacity than the full-length CON-S gp160 with all three MAbs tested (with b12 and F105 recognizing the CD4-binding site and 447-52D recognizing the anti-V3 loop). The M-TM.CT$_{MMTV}$ construct showed the highest antibody binding activity (Fig. 7E). Thus, chimeric Envs in VLPs retain conserved epitopes that are accessible to neutralizing antibodies.

DISCUSSION

To investigate determinants of Env assembly into VLPs, we compared a series of chimeric HIV-1 Env proteins with heterologous SP, TM, or CT sequences individually or in combination for their effects on Env incorporation into VLPs. We observed that substitution of the natural HIV SP with the mellitin SP resulted in a modest increase of both intracellular and cell surface expression of chimeric HIV-1 Con-S ΔCFI Env and resulted in an ~2-fold enhancement of its incorporation into VLPs, implicating a role of the SP sequence in the transport and assembly of membrane-anchored HIV Env proteins. In contrast, we did not observe significant effects of

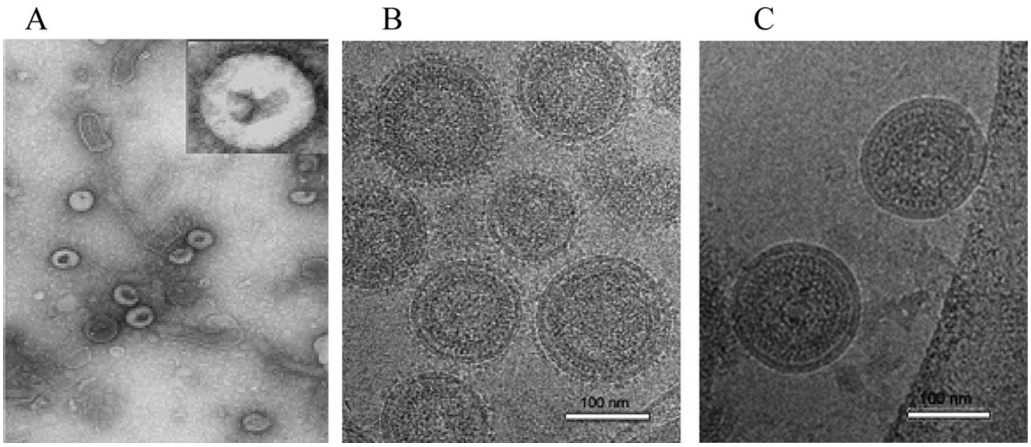

FIG. 6. Electron microscopy of HIV VLPs. (A) Conventional electron microscopy showing spherical VLPs negatively stained with sodium phosphotungstate with densely stained cores. Inset: enlarged (×5) to show some spike projections on the surface of VLPs. Magnification, ×40,000. (B) Cryo-electron microscopy showing intact chimeric Env-containing VLPs with surface projections. (C) Cryo-electron microscopy image of Gag VLPs lacking Env, showing a smooth surface. Magnification, ×135,000.

substitutions with either chitinase SP or BV gp64 SP compared to the parental HIV-1 Env construct.

The long CT domain of HIV-1 Env contains two cysteine residues (C764 and C837), which are targets for palmitoylation (32) and have been implicated in Env targeting to detergent-resistant lipid rafts, Env incorporation into the virus, and viral infectivity (3). It was also suggested that the full-length CT may play a regulatory role in limiting the amount of HIV-1 Env to 7 to 14 trimeric molecules per virion, since truncation of the CT increased Env incorporation by up to 10-fold (7). This is consistent with our observation that significant enhancement of Env incorporation into VLPs was achieved with Con-S ΔCFI Env and with chimeric constructs with a short heterologous CT or a complete deletion of the CT. However, Env with CT deleted was not found to be stably anchored into VLPs, since a significant amount of HIV-1 Env with CT deleted was lost after subsequent purification steps (G. Smith, unpublished observations). In contrast, Env fused to MMTV, HA, or BV gp64 TM-CT sequences showed more stable incorporation into VLPs. Therefore, although the CT sequence is not required for incorporation into virions, it may be important for stably anchoring the HIV-1 Env into the lipid bilayer of enveloped virus particles or VLPs.

We hypothesized that substitutions of HIV-1 Env TM-CT sequences with those from glycoproteins of other enveloped viruses (MMTV, LFV, BV, and influenza virus) would increase the level of Env incorporation into corresponding virus particles. MMTV and influenza virus can incorporate glycoproteins at levels up to 58 and 29% of total virion proteins, respectively (8, 30). The glycoproteins of these viruses have much shorter CT sequences than that of HIV-1 (Table 3). In our previous study, HIV VLPs were found to contain approximately 1.5% of Env when produced in BV expression system (28). In the present study, the highest level of Env incorporation into VLPs was observed with a chimeric construct with the MMTV TM-CT (M-TM.CT_{MMTV}) in which the molar ratio of Gag to Env was estimated to be 4:1, which is 14-fold higher than that observed with the full-length Con-S gp160 with a 56:1 ratio and 15-fold higher than that of HIV-1 virions with 60:1 ratio (7). Electron microscopy confirmed that the spherical VLPs exhibited protruding Env proteins on the surface. The chimeric HIV-1 Env construct with TM-CT sequences from BV gp64 was also found to be incorporated into VLPs at similarly high levels. Previously, segments of Env linked to the TM domain of the major Epstein-Barr virus envelope protein were also reported to be incorporated into VLPs at enhanced levels (10). These results indicate that the TM-CT sequences of viral glycoproteins play a role in determining the level of Env incorporation and suggest that the low level of incorporation of HIV Env into virions or VLPs is due, in large part, to a restriction imposed by the extended cytoplasmic domain.

Interestingly, a chimeric HIV-1 Env with a TM-CT sequence derived from the LFV GP protein was not effectively incorporated into VLPs despite its expression at high levels in insect cells. The arenavirus family, including LFV, has an unusually long and stable SP with a length of 58 aa which is known to be associated with the mature form of arenavirus gp (36) and could be important for assembly. The chimeric Env containing the influenza virus HA TM-CT sequences showed enhanced incorporation into VLPs, but at lower levels than found with the respective MMTV or gp64 sequences. Thus, specific structural features of the TM-CT sequences play a role in optimizing Env incorporation into released particles.

VLPs have been demonstrated to be potent HIV-1 candidate vaccines. Recent reports indicate that HIV Env-containing VLPs elicit both arms of immunity and induce specific immune responses at local and distal mucosal surfaces (4, 11, 12, 33). To elicit antibodies with broad neutralization capacity for genetically diverse HIV-1 isolates, it is important to design antigens in which the conserved neutralizing epitopes are exposed. Our studies show that HIV chimeric Env-containing VLPs, which are outfitted with heterologous TM-CT domains for enhanced particle incorporation, possess appropriate conformation of the cavity-laden CD4-gp120 interface, a conserved binding site for the chemokine receptor, and conserved epitopes for neutralizing antibody binding. Furthermore, these conserved regions are accessible in the VLPs. Therefore, chi-

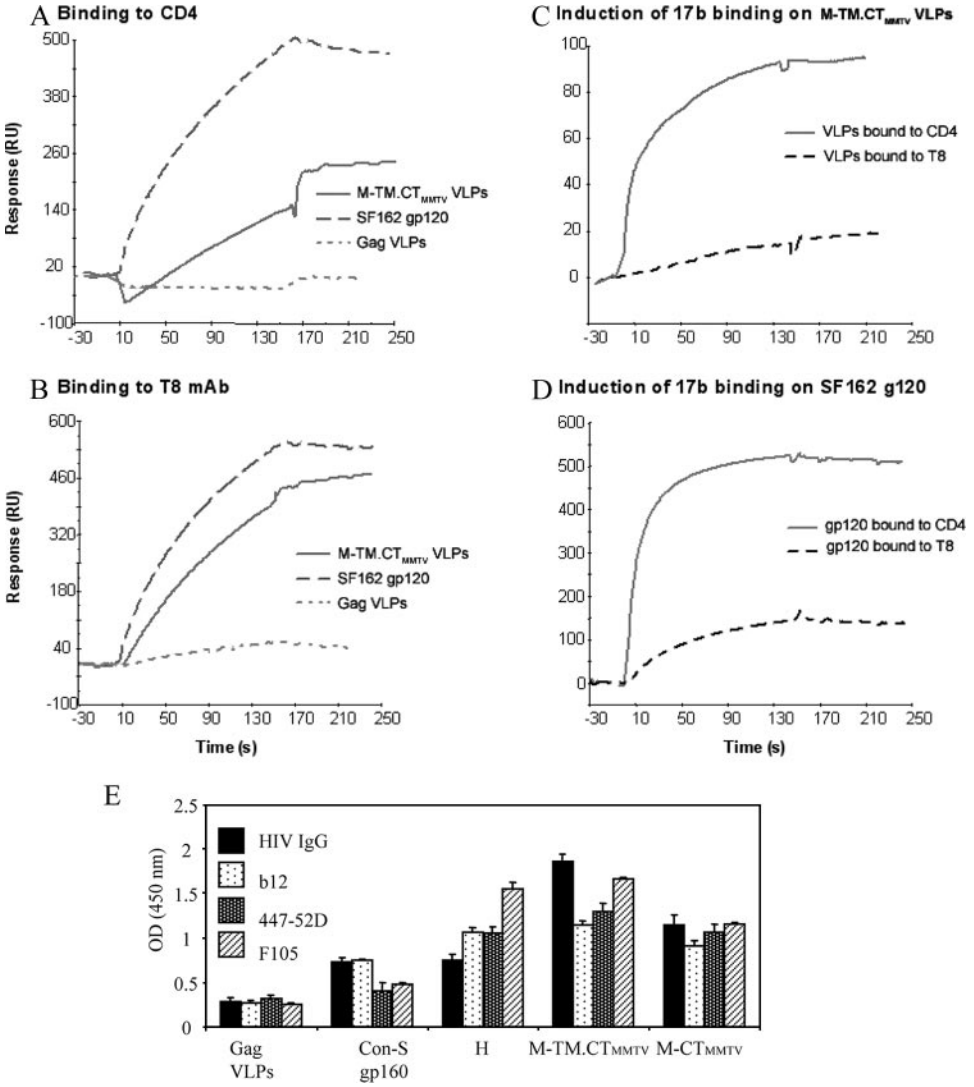

FIG. 7. Analysis of conserved antigenic regions on Env-enriched VLPs. For panels A to D, surface plasmon resonance assays performed as described in Materials and Methods. The VLP concentration used for binding was 1.25 mg/ml (Env level = 95 μg/ml). SF162 gp120 (150 μg/ml) was used as a positive control. For the detection of the ability of VLPs to bind to sCD4 or T8, sCD4 and T8 were covalently immobilized to a CM5 sensor chip (BIAcore), the VLPs or control was injected over each surface, and the binding was recorded. For determination of induction of 17b MAb binding, VLPs and control were captured on individual flow cells immobilized with sCD4 or T8. After stabilization of each surface, MAb 17b was injected and allowed to flow over each of the immobilized cells. (A and B) M-TM.CT$_{MMTV}$ VLPs binding to CD4 or T8 MAb, respectively. (C) MAb 17b binding to M-TM.CT$_{MMTV}$ after CD4 or T8 binding. (D) MAb 17b binding to SF162 gp120 after CD4 or T8 binding. (E) Binding of neutralizing antibodies to chimeric VLPs. Normalized VLPs (amount 0.05 μg of VLPs) were diluted to 100 μl and captured with anti-gp120 antibody-coated plates. Subsequently, Env-specific antibodies were applied, and binding was assayed by ELISA. HIV IgG, polyclonal IgG from HIV-infected patients; B12 and F105, MAbs recognizing CD4 binding site; 447-52D, MAb recognizing V3-loop. Goat anti-human IgG-HRP was used for detection. Representative data are shown from three independent experiments. Error bars represent the standard error.

meric VLPs with enhanced Env incorporation represent a promising immunogen for the development of an effective, safe AIDS vaccine.

ACKNOWLEDGMENTS

This study was supported by grants from the National Institutes of Health (P01 AI 28147 and P30 AI27767); a Collaboration for AIDS Vaccine Development grant to B.H.H. and B.F.H. from the Bill and Melinda Gates Foundation; and an internal directed research grant for vaccine design at Los Alamos National Laboratory.

We thank Bing Chen for helpful discussions, Derwei Venable for technical assistance, and Tanya Cassingham for preparation of the manuscript.

REFERENCES

1. **Barr, P. J., K. S. Steimer, E. A. Sabin, D. Parkes, C. George-Nascimento, J. C. Stephans, M. A. Powers, A. Gyenes, G. A. Van Nest, E. T. Miller, et al.** 1987. Antigenicity and immunogenicity of domains of the human immunodeficiency virus (HIV) envelope polypeptide expressed in the yeast *Saccharomyces cerevisiae*. Vaccine **5:**90–101.
2. **Benjamin, J., B. K. Ganser-Pornillos, W. F. Tivol, W. I. Sundquist, and G. J. Jensen.** 2005. Three-dimensional structure of HIV-1 virus-like particles by electron cryotomography. J. Mol. Biol. **346:**577–588.
3. **Bhattacharya, J., P. J. Peters, and P. R. Clapham.** 2004. Human immuno-

deficiency virus type 1 envelope glycoproteins that lack cytoplasmic domain cysteines: impact on association with membrane lipid rafts and incorporation onto budding virus particles. J. Virol. **78:**5500–5506.
4. **Buonaguro, L., L. Racioppi, M. L. Tornesello, C. Arra, M. L. Visciano, B. Biryahwaho, S. D. Sempala, G. Giraldo, and F. M. Buonaguro.** 2002. Induction of neutralizing antibodies and cytotoxic T lymphocytes in BALB/c mice immunized with virus-like particles presenting a gp120 molecule from a HIV-1 isolate of clade A. Antivir. Res. **54:**189–201.
5. **Chakrabarti, B. K., W. P. Kong, B. Y. Wu, Z. Y. Yang, J. Friborg, X. Ling, S. R. King, D. C. Montefiori, and G. J. Nabel.** 2002. Modifications of the human immunodeficiency virus envelope glycoprotein enhance immunogenicity for genetic immunization. J. Virol. **76:**5357–5368.
6. **Chakrabarti, S., M. Robert-Guroff, F. Wong-Staal, R. C. Gallo, and B. Moss.** 1986. Expression of the HTLV-III envelope gene by a recombinant vaccinia virus. Nature **320:**535–537.
7. **Chertova, E., J. W. Bess, Jr., B. J. Crise, Jr., I. R. Sowder, T. M. Schaden, J. M. Hilburn, J. A. Hoxie, R. E. Benveniste, J. D. Lifson, L. E. Henderson, and L. O. Arthur.** 2002. Envelope glycoprotein incorporation, not shedding of surface envelope glycoprotein (gp120/SU), Is the primary determinant of SU content of purified human immunodeficiency virus type 1 and simian immunodeficiency virus. J. Virol. **76:**5315–5325.
8. **Compans, R. W., H. D. Klenk, L. A. Caliguiri, and P. W. Choppin.** 1970. Influenza virus proteins. I. Analysis of polypeptides of the virion and identification of spike glycoproteins. Virology **42:**880–889.
9. **Demirov, D. G., and E. O. Freed.** 2004. Retrovirus budding. Virus Res. **106:**87–102.
10. **Deml, L., G. Kratochwil, N. Osterrieder, R. Knuchel, H. Wolf, and R. Wagner.** 1997. Increased incorporation of chimeric human immunodeficiency virus type 1 gp120 proteins into Pr55gag virus-like particles by an Epstein-Barr virus gp220/350-derived transmembrane domain. Virology **235:** 10–25.
11. **Deml, L., R. Schirmbeck, J. Reimann, H. Wolf, and R. Wagner.** 1997. Recombinant human immunodeficiency Pr55gag virus-like particles presenting chimeric envelope glycoproteins induce cytotoxic T cells and neutralizing antibodies. Virology **235:**26–39.
12. **Doan, L. X., M. Li, C. Chen, and Q. Yao.** 2005. Virus-like particles as HIV-1 vaccines. Rev. Med. Virol. **15:**75–88.
13. **Dokland, T., and M. L. Ng.** 2006. Electron microscopy of biology samples, p. 151–208. *In* T. Dokland, D. W. Hutmacher, M. L. Ng, and J. P. Schantz (ed.), Techniques in microscopy for biomedical application. World Scientific Press, Singapore.
14. **Eichler, R., T. Strecker, L. Kolesnikova, J. ter Meulen, W. Weissenhorn, S. Becker, H. D. Klenk, W. Garten, and O. Lenz.** 2004. Characterization of the Lassa virus matrix protein Z: electron microscopic study of virus-like particles and interaction with the nucleoprotein (NP). Virus Res. **100:**249–255.
15. **Freed, E. O.** 2002. Viral late domains. J. Virol. **76:**4679–4687.
16. **Fuller, S. D., T. Wilk, B. E. Gowen, H. G. Krausslich, and V. M. Vogt.** 1997. Cryo-electron microscopy reveals ordered domains in the immature HIV-1 particle. Curr. Biol. **7:**729–738.
17. **Ho, S. N., H. D. Hunt, R. M. Horton, J. K. Pullen, and L. R. Pease.** 1989. Site-directed mutagenesis by overlap extension using the polymerase chain reaction. Gene **77:**51–59.
18. **Hook, L. M., Y. Agafonova, S. R. Ross, S. J. Turner, and T. V. Golovkina.** 2000. Genetics of mouse mammary tumor virus-induced mammary tumors: linkage of tumor induction to the *gag* gene. J. Virol. **74:**8876–8883.
19. **Kang, S. M., F. S. Quan, C. Huang, L. Guo, L. Ye, C. Yang, and R. W. Compans.** 2005. Modified HIV envelope proteins with enhanced binding to neutralizing monoclonal antibodies. Virology **331:**20–32.
20. **Kieny, M. P., G. Rautmann, D. Schmitt, K. Dott, S. Wain-Hobson, M. Alizon, M. Girard, S. Chamaret, A. Laurent, L. Montagnier, and J.-P. Lecocq.** 1986. AIDS virus Env protein expressed from a recombinant vaccinia virus. Bio/Technology **4:**790–795.
21. **Lasky, L. A., J. E. Groopman, C. W. Fennie, P. M. Benz, D. J. Capon, D. J. Dowbenko, G. R. Nakamura, W. M. Nunes, M. E. Renz, and P. W. Berman.** 1986. Neutralization of the AIDS retrovirus by antibodies to a recombinant envelope glycoprotein. Science **233:**209–212.
22. **Li, Y., L. Luo, D. Y. Thomas, and C. Y. Kang.** 1994. Control of expression, glycosylation, and secretion of HIV-1 gp120 by homologous and heterologous signal sequences. Virology **204:**266–278.
23. **Liao, H. X., L. L. Sutherland, S. M. Xia, M. E. Brock, R. M. Scearce, S. Vanleeuwen, S. M. Alam, M. McAdams, E. A. Weaver, Z. Camacho, B. J. Ma, Y. Li, J. M. Decker, G. J. Nabel, D. C. Montefiori, B. H. Hahn, B. T. Korber, F. Gao, and B. F. Haynes.** 2006. A group M consensus envelope glycoprotein induces antibodies that neutralize subsets of subtype B and C HIV-1 primary viruses. Virology **353:**268–282.
24. **Lopez-Verges, S., G. Camus, G. Blot, R. Beauvoir, R. Benarous, and C. Berlioz-Torrent.** 2006. Tail-interacting protein TIP47 is a connector between Gag and Env and is required for Env incorporation into HIV-1 virions. Proc. Natl. Acad. Sci. USA **103:**14947–14952.
25. **Provitera, P., R. El-Maghrabi, and S. Scarlata.** 2006. The effect of HIV-1 Gag myristoylation on membrane binding. Biophys. Chem. **119:**23–32.
26. **Raghuraman, H., and A. Chattopadhyay.** 2004. Effect of micellar charge on the conformation and dynamics of melittin. Eur. Biophys. J. **33:**611–622.
27. **Saad, J. S., E. Loeliger, P. Luncsford, M. Liriano, J. Tai, A. Kim, J. Miller, A. Joshi, E. O. Freed, and M. F. Summers.** 2007. Point mutations in the HIV-1 matrix protein turn off the myristyl switch. J. Mol. Biol. **366:**574–585.
28. **Sailaja, G., I. Skountzou, F. S. Quan, R. W. Compans, and S. M. Kang.** 2007. Human immunodeficiency virus-like particles activate multiple types of immune cells. Virology **362:**331–341.
29. **Vzorov, A. N., and R. W. Compans.** 2000. Effect of the cytoplasmic domain of the simian immunodeficiency virus envelope protein on incorporation of heterologous envelope proteins and sensitivity to neutralization. J. Virol. **74:**8219–8225.
30. **Yagi, M. J., and R. W. Compans.** 1977. Structural components of mouse mammary tumor virus. I. Polypeptides of the virion. Virology **76:**751–766.
31. **Yamshchikov, G. V., G. D. Ritter, M. Vey, and R. W. Compans.** 1995. Assembly of SIV virus-like particles containing envelope proteins using a baculovirus expression system. Virology **214:**50–58.
32. **Yang, C., and R. W. Compans.** 1996. Palmitoylation of the murine leukemia virus envelope glycoprotein transmembrane subunits. Virology **221:**87–97.
33. **Yao, Q., Z. Bu, A. Vzorov, C. Yang, and R. W. Compans.** 2003. Virus-like particle and DNA-based candidate AIDS vaccines. Vaccine **21:**638–643.
34. **Yao, Q., F. M. Kuhlmann, R. Eller, R. W. Compans, and C. Chen.** 2000. Production and characterization of simian–human immunodeficiency virus-like particles. AIDS Res. Hum. Retrovir. **16:**227–236.
35. **Ye, L., Z. Bu, A. Vzorov, D. Taylor, R. W. Compans, and C. Yang.** 2004. Surface stability and immunogenicity of the human immunodeficiency virus envelope glycoprotein: role of the cytoplasmic domain. J. Virol. **78:**13409–13419.
36. **York, J., and J. H. Nunberg.** 2004. Role of hydrophobic residues in the central ectodomain of gp41 in maintaining the association between human immunodeficiency virus type 1 envelope glycoprotein subunits gp120 and gp41. J. Virol. **78:**4921–4926.
37. **Zingler, K., and D. R. Littman.** 1993. Truncation of the cytoplasmic domain of the simian immunodeficiency virus envelope glycoprotein increases env incorporation into particles and fusogenicity and infectivity. J. Virol. **67:** 2824–2831.